Turbidity Currents and Their Deposits

Eckart Meiburg

Department of Mechanical Engineering

University of California at Santa Barbara, Santa Barbara, CA 93106

email: meiburg@engineering.ucsb.edu

Ben Kneller

Department of Geology and Petroleum Geology

University of Aberdeen, Aberdeen AB24 3UE, UK

email: b.kneller@abdn.ac.uk

Key Words sediment transport, initiation mechanism, seafloor topography, erosion and deposition, linear stability, theoretical model

Abstract

The article surveys the current state of our understanding of turbidity currents, with an emphasis on their fluid mechanics. It highlights the significant role these currents play within the global sediment cycle, and their importance in environmental processes and in the formation of hydrocarbon reservoirs. Events and mechanisms governing the initiation of turbidity currents are reviewed, along with experimental observations and findings from field studies regarding their internal velocity and density structure. As turbidity currents propagate over the sea floor, they can trigger the evolution of a host of topographical features through the pro-

cesses of deposition and erosion, such as channels, levees and sediment waves. Potential linear instability mechanisms are discussed that may determine the spatial scales of these features. Finally, the hierarchy of available theoretical models for analyzing the dynamics of turbidity currents is outlined, ranging from dimensional analysis and box models to both depth-averaged and depth-resolving simulation approaches.

CONTENTS

1 Introduction

1.1 The Nature of Turbidity Currents

Turbidity currents are particle-laden gravity-driven underflows in which the particles are largely or wholly suspended by fluid turbulence. The turbulence is typically generated by the forward motion of the current along the lower boundary of the domain, the motion being in turn driven by the action of gravity on the density difference between the particle-fluid mixture and the ambient fluid. The ambient fluid is generally of similar composition to (and miscible with) the interstitial fluid, and in most natural cases on the Earth's surface is water. Turbidity currents are non-conservative in that they may exchange particles with a loose lower boundary (i.e. a sediment bed) by deposition or suspension, and may exchange fluid with the ambient by entrainment or detrainment. Such flows dissipate mainly through deposition of the particles. So long as the bed gradient is large enough that the turbulence generated by the forward motion of the current is sufficient to maintain the suspension, the current is said to be auto-suspending. Bagnold (1962), Pantin (1979) and others, reviewed by Pantin (2001) and Parker (1982) in a similar treatment, stressed the effects of entrainment of bed sediment into an auto-suspending current, which thus becomes catastrophically erosive, or 'ignitive' (see numerical treatment by Blanchette et al. (2005)).

Particle concentrations are often sufficiently low (0.1 - 7 % by volume) that particle-particle interactions play a small or negligible role in maintaining the suspension (Bagnold 1954) and from a modeling standpoint the Boussinesq approximation is commonly valid. Nonetheless, due to the extreme difficulty in estimating particle concentrations in natural flows in the ocean (see below) there remains considerable uncertainty - and debate - concerning the particle loading in large submarine turbidity currents.

1.2 The Concept of Turbidity Currents

The recognition of dense, sediment laden currents in Nature goes back to Forel (1885) who postulated that a subaqueous canyon in Lake Geneva had been created by underflows from the Rhone River. Daly (1936) suggested a similar mechanism for the formation of submarine canyons, and the name turbidity current was apparently coined by Johnson in 1939. However, the recognition of the nature of turbidity currents, and their potential importance in the transport of sediment to the deep sea (and in the formation of ancient sand layers that had previously been interpreted as shallow water deposits) is due to Kuenen (1938, 1951), Kuenen & Migliorini (1950) who conducted the first experiments on turbidity currents. That we still know so little of the nature and properties of natural turbidity currents can be ascribed to their infrequent and unpredictable occurrence, in remote and hostile environments (water hundreds to thousands of meters deep), and their destructive nature.

1.3 Significance

In a geophysical context, turbidity currents are important as agents of sediment transport into subaqueous environments such as deep lakes and oceans, and to some extent in the shallower seas of the continental shelves. In these situations the particles generally consist of rock or mineral fragment eroded from the land surface, transported by rivers to the shoreline, and re-sedimented into deeper water by turbidity currents. Calcium carbonate particles (mainly fragments of invertebrate shells) formed in shallow marine environments can be similarly re-sedimented into deeper water by turbidity currents. Indeed, turbidity currents, along with submarine landslides, are the principal means by which sediment is transported from shallower to deeper water. Transport distances range from a few hundreds of meters or less (for example down the submerged fronts of deltas) to thousands of kilometers on the ocean floor (e.g. North Atlantic Mid-Ocean Channel, Klaucke et al. (1998)).

Sediments in the deep sea and in deep lakes (e.g. Lake Baikal; Nelson et al. (1995)) are largely made up of turbidites, as the deposits of turbidity currents are known. Over periods of the order of 10^4 to 10^6 years these deposits may build up into vast sediment accumulations (submarine fans and related systems, Weimer & Slatt (2007)) with volumes up to millions of km^3 (e.g. Bengal Fan; Curray et al. (2003)). Ancient deposits of turbidite sand, deeply buried and compacted, form an important class of hydrocarbon reservoirs (Weimer & Slatt 2007), and the host rocks for a particular type of gold deposits (Keppie et al. 1987). Turbidity currents have also been invoked for the formation of banded iron formations, a type of iron ore deposit unique to the early history of the Earth (Lascelles 2007). In an environmental context, turbidity currents are responsible for much

of the sedimentation in reservoirs, e.g. De Cesare et al. (2001), Fan (1986), with consequent loss of water storage capacity. In the ocean, even rather small turbidity currents may damage or destroy sea-floor equipment and instrumentation, e.g. Inman et al. (1976), Khripounoff et al. (2003), Prior et al. (1987), and large currents commonly damage or remove sections of submarine cables (e.g. Dengler et al. (1984), Heezen & Ewing (1952)).

This article will cover initiation processes; the structure of turbidity currents as deduced from natural flows and experiments; the nature of their deposits; theoretical approaches to modeling; and some current controversies. It will not cover other types of particulate gravity currents such as pyroclastic flows, debris flows, rock avalanches, granular flows or snow avalanches. Various topics in gravity and turbidity current research have previously been reviewed. First and foremost, the book by Simpson (1997) offers a beautiful and accessible introduction to the field. The chapter by Rottman & Linden (2001) reviews the basic scaling laws and force balances for idealized compositional gravity currents. Several articles by Huppert review various aspects of gravity and turbidity currents. While Huppert (2000) provides a more general overview over topics related to gravity-driven geophysical flows, including the shallow water approach for analyzing them, Huppert (1998) focuses more exclusively on box models and shallow water equations for turbidity currents. Huppert (2006) discusses both dilute as well as concentrated particle-laden currents, along with dense granular flows. Middleton (1993) gives an elegant review of the literature on turbidity currents and their deposits, including experimental results and field data up to that time. Kneller & Buckee (2000) review experimental data and theory from a geological perspective. The recent article by Parsons et al. (2007) describes the range of sediment gravity

flows in the ocean, and to some degree we take this as our starting point, though offer a somewhat different perspective.

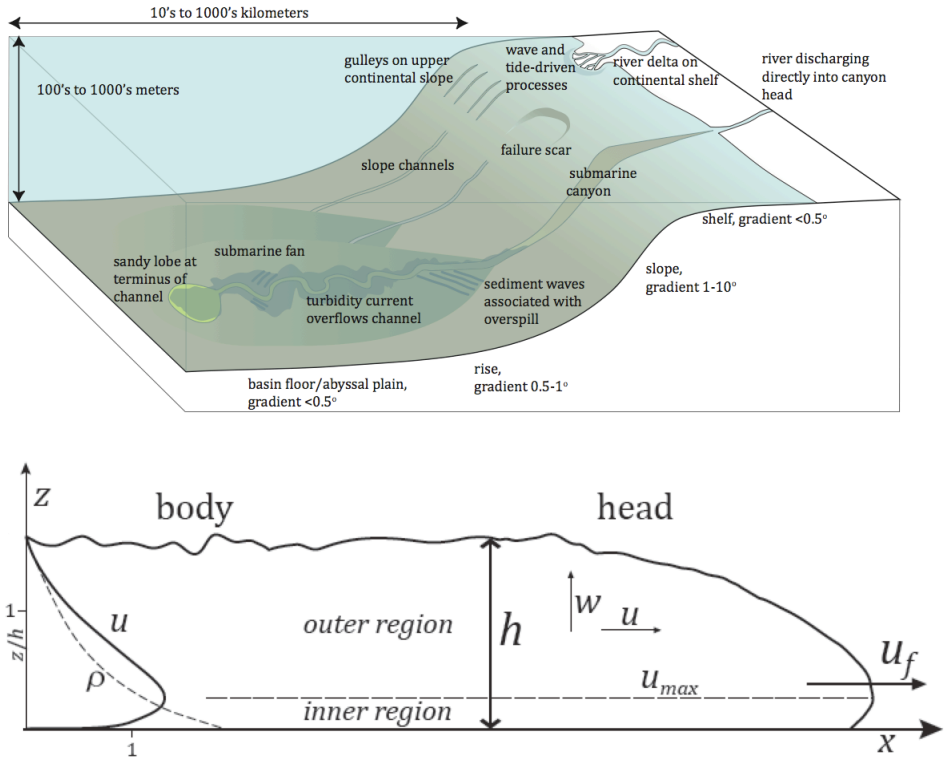

Figure 1: (a) Context of turbidity currents on the margins of continents and intra-continental basins, including deep lakes. (b) Schema of turbidity current showing generalized velocity and density profiles based on integral length scale for current thickness, $h = \frac{\int_0^\infty u dz}{\bar{u}}$ where $\bar{u} = \frac{\int_0^\infty u^2 dz}{\int_0^\infty u dz}$.

2 Simplified Theoretical Models

2.1 Dimensional Analysis

Much of the elegant experimental and theoretical research carried out over the last two decades by the groups at Cambridge, USC, UCSD and elsewhere demonstrates the ability of dimensional analysis to provide fundamental insight into the

dynamics of gravity and turbidity currents, cf. the partial reviews by Rottman & Linden (2001) and Huppert (2006). First and foremost, the celebrated result that the front velocity u_f of a gravity current of excess density $\Delta\rho$ in an ambient of density ρ_0 is proportional to the square root of the reduced gravity $g = g\,\Delta\rho/\rho_0$ and the front height h,

$$u_f \propto (g\,h)^{1/2} \tag{1}$$

follows from dimensional considerations of the balance between inertial and buoyancy forces alone. The classical analysis by Benjamin (1968) finds that the proportionality factor, commonly referred to as the Froude number Fr of the current, has a value of $\sqrt{2}$ for inviscid flows in deep ambients. A more recent, alternative theoretical treatment by Shin et al. (2004) yields $Fr = 1$. For environments of finite depth H, the experiments by Huppert & Simpson (1980) determine the dependence of Fr on the ratio h/H.

2.2 Box Models

For finite volume releases such as the classical lock-exchange configuration, conceptually simple box models can reproduce several aspects of experimentally observed flows (Huppert & Simpson 1980). These models neglect entrainment of ambient fluid and assume that the released fluid will evolve in the form of constant area rectangles, so that variations in the direction of the current are neglected. For gravity currents governed by a balance of gravitational and inertial forces, one finds that the front location evolves as $t^{2/3}$. This phase typically commences after the front has traveled $O(5-10)$ lock lengths at constant velocity (the so-called slumping phase). During the late stages of the flow, when viscous forces

become important, the front location depends on time as $t^{1/5}$. These scaling laws are in agreement with the experimental observations of Huppert (1982), Huppert & Simpson (1980), Rottman & Simpson (1983) and others. Dade & Huppert (1995), as well as Gladstone & Woods (2000) apply corresponding box models to particle-driven lock exchange flows, in order to obtain estimates of the current length vs. time. However, these authors also point out that the respective Fr-values depend on whether the interstitial fluid is fresh or saline, due to differences in the current shapes and structures.

2.3 Shallow Water Models

At the next level of complexity one finds so-called depth-averaged or shallow water models, first introduced for compositional gravity currents by Rottman & Simpson (1983), and later extended to turbidity currents by Bonnecaze et al. (1993) and by Parker et al. (1986). These models are reviewed in detail by Huppert (1998, 2006) and Parsons et al. (2007), so that we provide only a brief summary here. The shallow water approach typically neglects viscous forces and assumes that only small vertical accelerations are present, so that the pressure field is purely hydrostatic. At the top of the current, clear fluid is usually neither entrained nor detrained. Furthermore, the suspended phase is considered to be well-mixed across the height of the current, so that its volume fraction does not depend on the vertical location. This assumption may hold for very fine sediment, but it is questionable for coarser particles, or during the late stages of the flow when the decaying turbulence may no longer be fully able to distribute the particles across the entire current height. For the case of a deep ambient, the motion of the overlying fluid can be neglected, and the so-called single-layer shallow

water equations hold. For shallow ambients, on the other hand, it is necessary to extend this approach by formulating a two-layer system that also accounts for the dynamics of the overlying fluid layer (Baines 1995). We note that the equations for the conservation of the mass and momentum of the fluid, and of the particle volume fraction, have to be closed by prescribing the front velocity, which is commonly accomplished based on experimentally observed relationships between the current height, its reduced gravity, and its front velocity. Birman et al. (2009) employ a shallow water model for overflow currents in order to shed light on the processes governing the formation of levees. Their investigation shows the entrainment of ambient fluid to play an important role in determining the levee shape. While negligible entrainment rates lead to exponentially decaying levee shapes, constant entrainment rates result in power law shapes. Gonzalez-Juez & Meiburg (2009) extend earlier shallow water models by Lane-Serff et al. (1995) and references therein, in order to investigate gravity currents over submarine structures such as pipelines. Estimates of the maximum drag by the shallow water model are seen to lie within 10% of high resolution simulation results.

3 Field Observations

3.1 Natural Deposits

Erosion and deposition by turbidity currents are responsible for many of the features seen on the modern sea floor. Erosional features range from gulleys on the upper continental slope, a few tens of meters deep and hundreds of meters wide (see references in Hall et al. (2008)) to submarine canyons several kilometers wide and hundreds of meters deep, e.g. Inman et al. (1976), Weimer & Slatt (2007). Depositional features include laterally extensive, sheet-like deposits

of the abyssal plains, and also submarine fans, which are self-organized systems in many ways analogous to river deltas, similarly variable in form, and ranging from a few km to several thousand km across. Channels within these systems, tens to thousands of km in length, often have levees resembling those of river channels, formed analogously by overspill from the channel onto the adjacent sea floor; deposition within the channel and on the levees often results in elevation of the channel-levee system above the surrounding fan surface (Normark et al. 1997). The sediment bodies at the termini of these channels are typically lobate with extents of a few km^2 to a few hundred km^2, e.g. Deptuck et al. (20008) and references therein, and are largely deposited from unconfined flows, though some are apparently channelized to their margins (Twichell et al. 1995). The most continuous deposits often occur within bathymetrically confined regions on the sea floor small enough that turbidity currents may reach the confining topography (Gervais et al. 2006). Various bed-forms similar to those produced by unidirectional flow in shallow water may be produced by turbidity currents, especially within channels. Larger scale sediment waves may also be generated, especially where turbidity currents pass over topographic inflections such as the crests of submarine levees, or the base of the continental slope (where they may be associated with 'plunge pools'; Lee et al. (2002)), generating fields of sediment waves with heights of tens of meters, wavelengths O(1) km and crests oriented perpendicular to flow.

Our knowledge of these systems is based largely on observations on the modern sea floor, from side-looking sonar images, multi-beam bathymetry surveys, coring, shallow high-resolution seismic surveys, and increasingly from industrial seismic surveys, especially those used to assess sea-floor hazards to drilling. Outcrops

of ancient turbidites have generated numerous qualitative models, and much a posteriori reasoning about the nature of the flows responsible, e.g. Mulder & Alexander (2001). In a fluid mechanical context, they offer the prospect of providing benchmarking data for future numerical simulations.

3.2 Data From Natural Flows: Scale, Dynamics and Flow Structure

Few turbidity currents in the ocean have provided much evidence of the nature of the flows themselves, and much of that evidence has until recently been indirect. Most widely known is the event of November 18, 1929, off the Grand Banks of Newfoundland (Piper et al. (1999) and references therein). This followed a magnitude 7.2 earthquake beneath the upper continental slope at 500 to 700 m water depth, accompanied by numerous sea-floor failures and submarine cable breaks in the epicentral region; a number of cable breaks occurred in sequence down the continental slope over the ensuing thirteen hours. The total failed volume was perhaps 100 km^3 consisting mainly of silt and clay. Some of the failed material transformed into turbidity currents flowing down the slope valleys, which eroded some 50 to 100 km^3 of sand that had accumulated over the past 10,000 years or so. Increasing wavelengths of bedforms down the first 100 km of the valley indicate an accelerating (ignitive) current, despite a decrease in gradient from 8^o to 1^o. Below about 4700 m water depth the bed is depositional, probably triggered by the radial expansion of the flow as it began to exit the valley; on the northern part of the abyssal plain the deposit (mainly of fine sand) is $> 1m$ thick, extending 450 km and becoming thinner and finer rapidly at its margins. The deposit covers an area roughly the size of Texas, with a volume estimated as 150

to 175 km^3, of which perhaps only 10 km^3 is mud (fine silt and clay); the missing mud was probably carried away by deep-ocean circulation. The maximum front velocity, estimated from the timing of cable breaks, was c. 19 m s^{-1}. Indirect estimates of maximum flow thickness range from 300 to 400 m. This suggests overall Reynolds numbers of $O(10^9 - 10^{10})$ on the slope.

An event involving the failure of at least 8 x 10^6 m^3 of land-fill material occurred near the mouth of the Var River SE, France, in 1979 (Dan et al. 2007). This generated a turbidity current $O(10^2)$ m thick that severed submarine cables, the first, located at 95 km from the source, was cut 3 h 45 min after the initial failure (indicating an average head speed of 7.4 ms^{-1}), the second cable, situated at 122 km, was cut after 8 h (1.74 ms^{-1}, over a 0.15^o slope Piper & Savoye (1993).

Turbidity currents on the Congo-Zaire submarine fan have been inferred from cable breaks to occur every one or two years (Khripounoff et al. (2003) and references therein). Recent direct observations recorded a flow through a submarine fan channel at $4000m$ water depth, carrying sand and plant debris, attaining velocities $> 1.2ms^{-1}$ at 150 m above the channel floor, and overflowing onto the surrounding sea bed at least 18 km from the channel. A cloud of suspended mud persisted at the site for several months. The current was unrelated to flooding in the Congo River. Frequent turbidity currents occur in Bute Inlet, a British Columbia fjord, associated with late spring to summer floods (Prior et al. 1987). Maximum velocities are > 3.35 m s^{-1} measured 4 m above the fjord floor, with coarse sand suspended at heights of at least 6 to 7.5 m and total flow thicknesses of more than 30 m. The currents flow at least 25 km along the fjord, and possibly as far as 40 to 50 km, over bottom slopes of generally less than 1^o.

The most complete picture of any marine currents to date comes from Monterey Canyon, California. Vertical profiles of down-stream velocity were measured by Xu et al. (2004) for four flows over the space of a year, at three locations down the canyon ($1450m$, $2837m$ and $3223m$ water depth). Two of the four flows were storm-generated; none was seismically triggered. Peak velocities (averaged over an hour) were from c. 0.5 to 2 ms^{-1}. Flow thickness increased down-canyon, and the height of the velocity maximum decreased down-canyon. The flows persisted for several hours each, but the duration of peak flow decreased down-canyon and became more surge-like. Measurements in lakes and reservoirs have been made by, inter alia, Best et al. (2005), Chikita (1989), Gould (1951), Normark (1989). Normark and Best et al. both noted the development of pulsing flow with periods of a few minutes, despite steady inflow conditions.

4 Flow Structure

Turbidity currents can be differentiated into a front region (or 'head') and body (figure 1b). As shown above, the rate of advance of the front is found to be virtually independent of the lower boundary slope. The motion of the fluid behind the head can be approximated with a modified form of the Chezy equation for flow in open channels, using the reduced gravity (Middleton 1993), and is slope dependent. Consequently, the buoyancy flux into the head increases with increasing slope, with a concomitant effect on mixing (see below). Finite-volume releases ('surge-type' currents) may be dominated by the properties of the front (Hacker et al. 1996), in contrast to sustained or continuous underflows.

4.1 Velocity and Turbulence

The vertical structure of density and turbidity currents is analyzed by Stacey & Brown (1988). The mean velocity structure of turbidity currents consists of an inner (near-wall) region with a positive velocity gradient, similar to a conventional turbulent boundary layer, and an outer region (shear layer), generally five to ten (or more) times thicker than the inner region, with a negative velocity gradient and shear stress of opposite sign (figure 1b). The velocity structure has been compared to that of plane turbulent wall jets (Kneller & Buckee (2000), Parker et al. (1987) and references therein, Gray et al. (2005), Leeder et al. (2005)). However, the use of $y^{1/2}$ (the height at which the downstream velocity falls to half its maximum), advocated by Launder & Rodi (1983) as a characteristic length scale for wall jets, yields a rather unsatisfactory collapse of velocity profiles compiled from different contexts (Kneller & Buckee (2000), see also Gray et al. (2005)), suggesting that the shear layer deviates from a Gaussian profile. In fact for some currents the shear layer profile is close to linear (Ellison & Turner (1959), Xu et al. (2004)).

Turbulent kinetic energy profiles in turbidity currents are similar to those of saline gravity currents, being close to zero at the height of the downstream velocity maximum (Gray et al. (2005), Kneller et al. (1999), Kneller & Buckee (2000), Leeder et al. (2005)) reflecting the dominance of turbulence production by shear related to the mean stream-wise velocity profile.

4.2 Density

The density structure is determined in the case of simple turbidity currents (i.e. those in which the interstitial and ambient fluids are of the same density) by the

distribution of suspended sediment. Many authors have shown that the highest suspended sediment concentrations (and commonly the steepest gradients in concentration) occur immediately above the bed (figure 1b; see review in Kneller & Buckee (2000)). Parker et al. (1987) found the vertical distribution of suspended sediment to have a much weaker dependence on the ratio of the shear velocity to the sediment fall velocity than is the case in open-channel suspensions. Baas et al. (2005) showed that suspended sediment distribution is highly unsteady, and considered it to be controlled largely by the ratio of particle settling velocity to the upward-directed components of local turbulent velocity associated with coherent flow structures. Leeder et al. (2005) proposed a criterion for the maintenance of suspension based on the ratio of maximum vertical turbulent stress to immersed weight of suspended load over unit bed area.

4.3 Entrainment

Entrainment of ambient fluid into the head of gravity currents is shown by Parsons & Garcia (1998) to be dependent on a Reynolds number based on the cube root of the buoyancy flux into the head. Entrainment into the body is a function of the overall Richardson number, Ellison & Turner (1959)). Parker et al. (1987), based on experiments with turbidity currents, propose an empirical relation

$$e_w = 0.075/(1 + 718Ri^{2.4})^{0.5} \tag{2}$$

where

$$Ri = \frac{hg(\frac{\Delta\rho}{\rho})}{u^2} \tag{3}$$

in which e_w is the entrainment coefficient (entrainment velocity normalized by

mean downstream velocity), h is the current height, and u the mean stream-wise velocity.

Evidence of very low entrainment rates on the ocean floor (Birman et al. (2009), Srivatsan et al. (2004)), borne out by extremely long run-out distances of channelized flows, suggests high Richardson numbers and thus sub-critical flow on the low gradients of basin floors (in contrast to flows on continental slopes; Parsons et al. (2007)). This argues for stable density stratification in the shear layer, i.e. gradient Richardson numbers, Ri, sufficiently above the critical value of 0.25 to suppress mixing

$$Ri_g = \frac{(g\frac{\partial\rho/\partial z}{\rho_o})}{(\partial u/\partial z)^2} \tag{4}$$

where z is the vertical co-ordinate. Various authors have investigated the flow of turbidity currents into confining topography, where the flow thickness and topographic height control the interaction (Brunt et al. (2004), Lamb et al. (2004)), and also the effects of gradient changes on flow behavior and deposition (Garcia & Parker 1993) concluding that hydraulic jumps need not occur (Gray et al. 2005) but where they do they may generate upstream facing steps (Kostic & Parker (2006)). The effects of reversing buoyancy were reviewed by Kneller & Buckee (2000) and references therein. The turbulence structure of lofting flows was recently investigated by Al-Musallami & Al-Ja'aidi (2008).

In summary, the above observations of a complex internal flow structure suggest that high-resolution simulations of turbidity currents can provide insight beyond that gained from simplified theoretical models.

5 Depth-Resolving Numerical Simulations

Over the last decade, large-scale, depth-resolving simulations have begun to contribute to our understanding of gravity and turbidity currents. Perhaps the first highly resolved DNS simulation of compositional gravity currents was conducted by Härtel et al. (2000) for the lock-exchange configuration, cf. also Ooi et al. (2007) and Cantero et al. (2007). More recently, highly resolved simulations have also been conducted for particulate gravity currents. Towards this end, Felix (2002) introduces a two-dimensional Reynolds-averaged model for a boundary layer approximation of the Navier-Stokes equations. He employs this model to simulate several large-scale historical turbidity currents, such as the Bute Inlet and Grand Banks flows. A similar approach is taken by Kassem & Imran (2004), and by Huang et al. (2005), whose simulations are reviewed in detail by Parsons et al. (2007). These authors employ a finite volume model on a grid that is recalculated after every time step in order to allow for the temporal variation of the bottom topography in response to erosion and deposition. This is a costly approach; in general it may more promising to employ a grid that does not change with time, and to represent the evolving bottom topography via an immersed boundary approach (Mittal & Iaccarino 2005).

In order to avoid the uncertainties associated with determining empirical constants in RANS models, Necker et al. (2002) explore much smaller, laboratory-scale flows in the lock-exchange configuration via highly-resolved, three-dimensional direct numerical simulations (DNS) (figure 2b). The authors consider dilute distributions of particles with negligible inertia that are smaller than the smallest length scales of the buoyancy-induced fluid motion. The suspended phase is described in an Eulerian fashion, via a convection-diffusion equation for the local

particle number density.

The authors observe that in three-dimensionally evolving currents, particles sediment out more rapidly than in their two-dimensional counterparts, which points to the important role played by spanwise instabilities. Regarding the final deposit profile, they observe excellent agreement with corresponding laboratory data of De Rooij & Dalziel (1998). Such high-resolution, DNS simulations can be interrogated for quantitative information that is not readily accessible experimentally, such as energy budgets. Surprisingly, the authors observe that over a wide range of parameters roughly half of the initial potential energy is lost in the small scale Stokes flows around the sedimenting particles, so that it is not available for convective transport and mixing. While the simulations by Necker et al. (2002) do not account for erosion and resuspension, they demonstrate that the largest shear stresses are exerted on the bottom walls initially by the large-scale spanwise Kelvin-Helmholtz rollers, and later by the lobe-and cleft structures at the front.

In a follow-up study, Necker et al. (2005) analyze the differences between shallow and deep-water flows with regard to the energy budgets and mixing behavior. Blanchette et al. (2006, 2005) further extend this line of work to eroding and resuspending turbidity currents, based on the experimentally measured relationship (Garcia & Parker 1993) between particle flux, bed shear stress, settling velocity and particle Reynolds number. They observe that particles eroded over the length of the current are transferred to the current head, where they can lead to an acceleration of the flow, thus increasing the local bed shear stress and potentially rendering the current self-sustaining. In spite of the availability of experimental correlations, the detailed mechanisms by which a current detaches

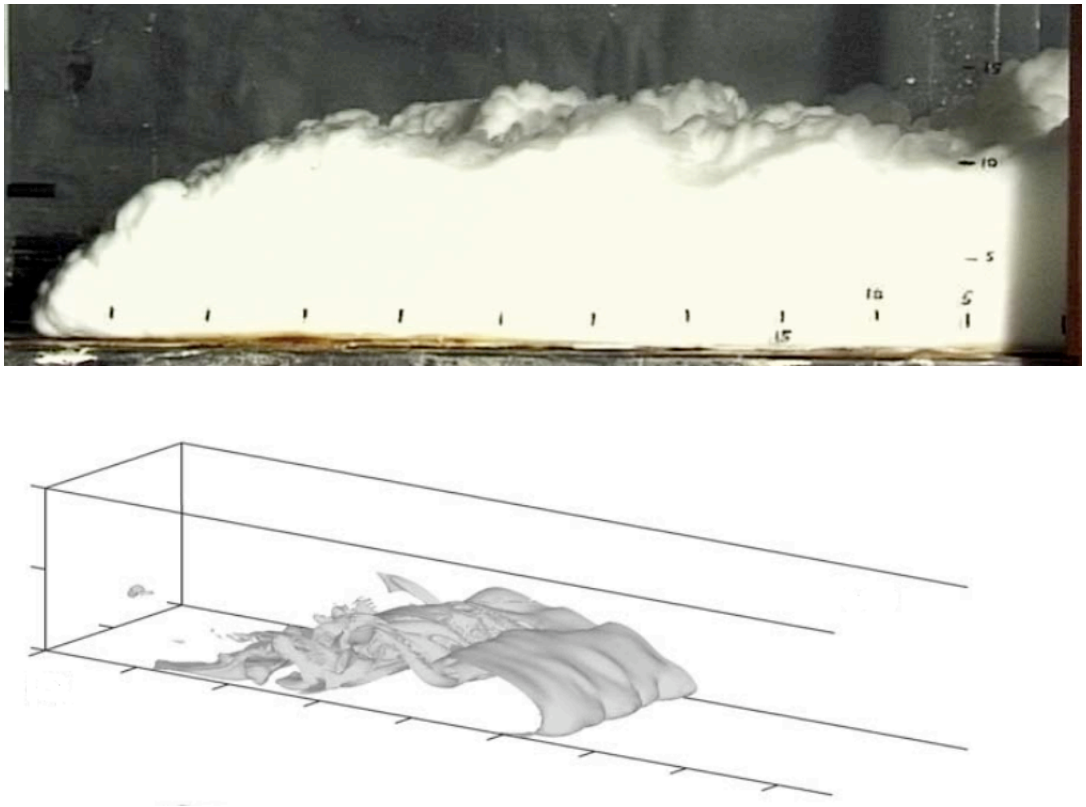

Figure 2: (a) Experimental turbidity current front in the laboratory, showing the overhanging 'nose' that corresponds to the height of the stream-wise velocity maximum. Scale in cm. From Baas et al. (2005). (b) DNS simulation of a turbidity current (from Necker et al. (2002)). The current structure is visualized by an isosurface of the concentration field.

individual grains from a sediment bed are still poorly understood. Boegman & Ivey (2009) argue that not just the shear stress at the bed surface, but also the structure of the flow field above is crucial for lifting particles from the bed. In addition, the coupling between coherent structures within the turbidity current and corresponding features in the porous sediment bed below gives rise to interesting questions that are currently wide open. Some hope derives from recent advances in the computational modeling of flows with many suspended particles (Pan et al.

(2002) and references therein), which hopefully will soon allow for detailed simulations of the detachment process. An extension of the numerical methodology for treating dilute suspensions containing particles with weak inertia is developed by Ferry & Balachandar (2001), by means of an expansion of the particle velocity field in the dimensionless particle response time (Stokes number). This allows for an Eulerian treatment of the particle velocity field that is able to capture such effects as sedimenting particle ejection from vortex cores and particle trapping in stretched vortices (Marcu & Meiburg (1996), Marcu et al. (1995), Martin & Meiburg (1994), Raju & Meiburg (1995)). Very recently, this approach has been applied to turbidity currents by Cantero et al. (2008). While the above simulations account for suspended sediment only, bedload transport is known to play an important role as well in many flows, especially in determining the character of the final deposit. In a recent investigation, Schmeeckle & Nelson (2003) develop a computational model for bedload transport by tracking large numbers of individual particles based on a variant of the equation derived by Maxey & Riley (1983). Interactions among particles, including collisions, are modeled as well. Keeping in mind the fairly restrictive limitations under which the Maxey-Riley equation holds, it may be attractive to base future detailed models on full Navier-Stokes simulations of many particle suspensions. Simulations along these lines open up the interesting opportunity to obtain direct information about a variety of properties of the sediment bed, among them the spatially varying distribution of particle sizes, porosity and permeability. Such information will be extremely valuable in building hydrocarbon reservoir models.

A practical concern lies in the potentially destructive impact of gravity and turbidity currents on submarines installations such as pipelines and well heads.

Gonzalez-Juez et al. (2008b) perform two-dimensional Navier-Stokes simulations for such flows around circular cylinders mounted above a wall. Their simulations confirm the experimentally observed impact, transient and quasisteady stages (Ermanyuk & Gavrilov (2005)), and provide insight into the mechanisms linking flow structures to unsteady lift and drag forces. The investigations by Gonzalez-Juez et al. (2008a) and Gonzalez-Juez & Meiburg (2009) extend this line of work to three-dimensional flows, rectangular shapes, as well as bottom shear stress and scour information.

Frequently, there exists considerable uncertainty regarding the formulation of realistic initial conditions in numerical simulations of turbidity currents. This represents the motivation for taking a closer look at the mechanisms responsible for triggering such flows.

6 Initiation Mechanisms

6.1 Sediment failure

The initiation of turbidity currents depends on the formation of a sediment suspension. Since the 1950's it has been recognized that turbidity currents can be initiated by sediment failures on the slope (e.g. Gorsline et al. (2000), Heezen & Ewing (1952)); this occurs through the dilution and transformation of the resulting submarine landslides or debris flows (Hampton (1972), Normark & Piper (1991), Parsons et al. (2007)). More recent work has evaluated the mechanisms of this transition, which occurs either by shearing or detachment of material from the surface of the debris flow, or by the initiation of turbulence within the body of the flow which depends upon a critical ratio of dynamic stress to shear strength, in turn dependent on the proportion and type of clay present (Felix & Peakall

(2006), Marr et al. (2001), Mohrig & Marr (2003)). Many such submarine failures are initiated by earthquakes (Gutierrez-Pastor et al. (2009), Heezen & Ewing (1952)), but in some cases simply result from deposition on a slope, leading to oversteepening and failure(Girardclos et al. 2007).

6.2 Rivers, flood and storms

The generation of turbidity currents has also been attributed to rivers in flood. Suspended sediment concentrations in river outflows are typically up to a few kg per m^3, falling to a few g per m^3 in the far field (e.g. Zaire River, Eisma & Kalf (1984); Amazon River, Rockwell Geyer & Kineke (1995)). In plumes generated by river outflows into freshwater lakes, the contribution of suspended sediment to the (negative) buoyancy is of the same order as that due to temperature differences, and river-generated underflows (so-called hyperpycnal flows) are common (e.g. De Cesare et al. (2001), Lambert & Giovanoli (1988)), especially during floods, when suspended sediment concentrations are high (Nash 1994). River plumes discharging into the ocean are typically positively buoyant since the density difference due to salinity normally greatly exceeds the density contribution due to suspended sediment. Sedimentation from such plumes may generate turbidity currents in either of two ways.

Firstly sediment may settle convectively from the plume at rates up to two orders of magnitude higher than Stokes settling velocities (McCool & Parsons 2001), and generate a bottom-propagating turbidity current (Maxworthy (1999), Parsons et al. (2001, 2007); see below); simple scaling relations predict sediment settling velocities in agreement with those of sediment from a natural river plume (Eel River, California; McCool & Parsons (2001)). Maxworthy (1999) finds the

surface current to behave quite similarly to a non-particulate current of equal density. In certain parameter ranges, however, the evolution of the current is strongly affected by the loss of particles and interstitial fluid at its lower boundary, which translates into a loss of momentum and an effective retarding stress. After an initial constant velocity phase, the current begins to slow down as a result of this loss of momentum, until it comes to a complete stop. Simultaneously, vigorous plumes containing particles, interstitial and ambient fluid develop at the underside of the current. Upon reaching the floor of the experimental tank, they form a secondary turbidity current propagating horizontally along this wall. This secondary current still contains some of the interstitial fluid that was dragged downwards by the particles. This interstitial fluid is subsequently released from the secondary turbidity current through upward moving plumes. The surface current, after having lost most of its particular matter, eventually becomes sufficiently buoyant to start moving forward again. Maxworthy (op cit) presents scaling arguments for both the early, intermediate and late stages of the flow.

A second mechanism involves the re-suspension of muddy sediment lost from the plume at or close to the river mouth due to flow expansion, and the rapid decay of bottom-generated turbulence where the plume detaches from the sea bed at a saline front; this may be combined with flocculation of clays on contact with salt water, leading to rapid sedimentation and the formation of fluid muds (dense suspensions with $> 10 kgm^{-3}$ of sediment; e.g. Kineke & Sternberg (1995)). The slopes of most continental shelves are too low to sustain auto-suspension (Wright & Friedrichs (2006)), but tidal currents (Ogston et al. (2008), Wright et al. (1990)) or waves (Traykovski et al. (2000), Warrick et al. (2008)) may generate turbu-

lence sufficient to maintain this sediment in suspension, or to re-suspend it after a short period of residence (hours to months) on the continental shelf (Palanques et al. (2006a), Warrick et al. (2008)); once suspended it moves across the low gradient of the shelf as a hybrid gravity current, to be re-deposited further out on the shelf, or eventually to find its way into deeper water (Wright & Friedrichs 2006). These mechanisms have recently been extensively reviewed by Parsons et al. (2007).

However, the high suspended sediment loads developed during river floods may occasionally lead to river discharges whose bulk density exceeds that of coastal waters (circa 1025 - 1030 $kg\ m^3$), producing a sediment-laden underflow. Such events have been recorded historically, most notably in Taiwan (Dadson et al. (2005), Milliman & Kao (2005)), and implied elsewhere (Mulder et al. (2003)). Their frequency has been predicted on the basis of historic data for river discharge and suspended sediment load (Mulder & Syvitski 1995). With the present hydrologic regime and sea level they are restricted to few a rivers with large ranges in discharge, which drain elevated and/or easily erodible catchments; this excludes the worlds largest rivers.

Except where discharging directly into a canyon head, high suspended sediment concentrations in rivers are generally insufficient on their own to generate hyperpycnal currents (Warrick et al. (2008), Wright et al. (1990)). Elsewhere, a contribution from waves or tides is necessary to maintain the sediment in suspension or re-suspend it as it traverses the shelf (Palanques et al. 2006a). Even where wave action is a result of the same storm that generated the flood, the cross-shelf transit leads to a delay of hours to days before the turbidity current can be detected in the canyon. This is so even where the river mouth is only a few

kilometers from the canyon head (e.g. Salinas and Santa Clara rivers, California; Warrick et al. (2008), Xu et al. (2004)); nonetheless, the interstitial water in the current is typically warmer and less saline than the ambient seawater, implying that river water is involved and the cross-shelf gravity flow has maintained some integrity.

The generation of hyperpycnal currents has occasionally been detected where the river outflow discharges directly into the head of a submarine canyon (Kuehl et al. 2004), a situation more common at times of lowered sea level (most recently during Pleistocene glacial periods) when rivers discharge directly to the top of the continental slope. The transfer of sediment to the deep sea by turbidity currents, generated by this and other mechanisms, is held to have been far more frequent during such sea level low-stands (Weimer & Slatt (2007), Blum & Hattier-Womack (2009) in press).

Storms are implicated in other mechanisms of turbidity current generation, on coastlines with both wide and narrow shelves. Down-welling is a phenomenon associated with strong onshore winds that produce a set-up (a piling up of water at the shoreline) that results in a deep offshore counter-flow; in summer, when sea water is stratified, down-welling is inhibited by buoyancy, but in winter, when water is well-mixed and of homogeneous density, winter storm-induced down-welling flow (occurring every few years) may suspend sufficient sediment to become gravity-driven and auto-suspending on steeper slopes (Palanques et al. 2006a). Down-welling may also be a mechanism by which tropical storms generate turbidity currents (Dengler et al. 1984). Sustained cold winter winds can also generate cold dense water on the shelf that cascades down the slope, flushing sediment out of submarine canyons en route, in events lasting from a few hours

to a week (e.g. Gulf of Lions, Canals et al. (2006)).

Yet another mechanism may occur when canyons cut close to the shoreline, where wind and wave set-up, possibly combined with standing edge waves (all of which are associated with high winds and waves) produce oscillations with a dominant down-canyon component; when sand is present in the canyon head (supplied by long-shore currents) these oscillations culminate in an energetic down canyon current. This situation was described in detail for the Scripps Canyon, California, by Inman et al. (1976). Sediment in canyon heads or gulleys on the upper slope that acts as 'fuel' for turbidity currents is commonly supplied by wind and tide driven currents, to be subsequently remobilized by turbidity currents. Mastbergen & Van Der Berg (2003) suggest that progressive retreat of steep failure-generated slopes in fine sands (a process known as breaching) may be instrumental in the generation of sustained turbidity currents during the flushing of canyons.

6.3 Other mechanisms

Other, non-meteorological events on land may also be linked to the formation of turbidity currents. Earthquake-triggered subaerial landslides can introduce large quantities of sediment into river systems (Dadson et al. 2005). The breaching of glacially-dammed lakes may also generate turbidites via catastrophic floods (Brunner et al. 1999). Volcanically-triggered sub-glacial lake breakouts (jokulhlaups) constitute a special case of such events, which may also generate turbidity currents when they enter the ocean (Geirsdóttir et al. 2000). Volcanic eruptions can generate turbidity currents directly when pyroclastic flows enter the sea (Trofimovs et al. 2008), or indirectly when ash falls and pyroclastic flows

introduce large quantities of ash into river systems; eruptions are often accompanied by high rainfall associated with eruption column convection, leading to floods with extremely high suspended sediment discharges that form hyperpycnal flows on entering the ocean (Nelson et al. 1988).

Anthropogenic turbidity currents include the effects of mine tailings being dumped into Lake Superior (Normark 1989); land-fill, such as may have contributed to the Var turbidity current in 1979 (Dan et al. 2007); dumping of dredged material at a canyon head (Xu et al. 2004); and trawling along a canyon wall (Palanques et al. 2006b).

7 Turbidity Current/Sediment Bed Interaction

Since the channels and gullies created by turbidity currents play an important role as pathways for sediment transport down the continental slope, it is desirable to obtain insight into the processes underlying their formation (Parsons et al. 2007). Interestingly, gullies, channels, sediment waves and other features on the sea floor frequently appear in straight, evenly spaced patterns, which suggests the presence of an underlying, coupled hydrodynamic/sediment-driven instability. The hypothesis of an instability mechanism at the heart of submarine channel inception has spawned a number of investigations employing depth-averaged flow and sediment transport models, starting with the classical work of Smith & Bretherton (1972), cf. also the references in Parsons et al. (2007) and Hall et al. (2008).

A disadvantage of depth-averaged approaches in this regard lies in their inability to capture the detailed interaction between the sediment bed and the three-dimensional flow structures above. Specifically, potential coupling mechanisms between the spanwise and vertical velocity components on one hand, and the ero-

sion process on the other, cannot be explored with this approach. Colombini & Parker (1995) show such coupling mechanisms to be important with regard to the formation of longitudinal topographical features by bedload transport. A related experimental investigation is conducted by Wang & Cheng (2005). Colombini & Parker (1995) further elaborate on this concept with a view towards generating small amplitude 'streak' features of a few grain diameters.

The recent investigation by Hall et al. (2008) aims to explore the importance of two-way coupling mechanisms between transverse turbidity current flow structures and suspended sediment for the formation of submarine gullies and channels. Towards this end, the authors conduct a linear stability analysis based on the full three-dimensional Navier-Stokes equations, rather than depth-averaged equations. They identify a conceptually simple and physically intuitive stability criterion which states that, for instability to occur, the suspended sediment concentration of the base flow needs to decay more slowly away from the sediment bed than does the shear stress inside the current. Under such conditions, an upward protrusion of the sediment bed will find itself in an environment where erosion decays more quickly than sedimentation, so that it will keep growing. The authors show that this destabilizing effect of the base flow is modulated by the stabilizing perturbation of the suspended sediment concentration, and by the shear stress due to a secondary flow structure in the form of counter-rotating streamwise vortices. As pointed out by Nielsen & Teakle (2004), measurements in river flows over bedforms typically show sediment diffusivities that are larger than the eddy viscosities, so that the conditions for instability are satisfied. For a representative current height of O(10-100m), the linear stability analysis provides a most amplified wavelength in the range of 250-2,500m, which is consistent

with field observations reported in the literature. The above Navier-Stokes based analysis could serve as a starting point for a secondary instability analysis to gain insight into the frequently observed meandering evolution of submarine channels, cf. also the nonlinear model by Imran et al. (1999), and the experiments by Yu et al. (2006), which are the first to report channelization by turbidity currents and mudflows at the laboratory scale.

Interestingly, the base flow instability mechanism identified by Hall et al. (2008) should also apply to the formation of streamwise sediment waves by turbidity currents and bottom flows carrying suspended sediment. This hypothesis is borne out by the linear stability analysis of Hall 2009 (personal communication). Their results confirm the earlier analysis by Flood (1988), who links the formation of sediment waves to the presence of internal waves in the density-stratified region above the sediment bed, cf. also the analysis of lee waves by Queney (1948). For supercritical flows over an erodible bed, Parker & Izumi (2000) propose an alternative mechanism for the generation of streamwise periodic structures, so-called cyclic steps. Their analysis, based on the shallow water equations, demonstrates the evolution of slowly upstream migrating features, each of which is associated with a headcut and a related hydraulic jump. Laboratory experiments demonstrating this mechanism are presented by Taki & Parker (2005), while Sun & Parker (2005) discuss corresponding nonlinear shallow water simulations.

8 Outlook and Open Questions

Experimental investigations of turbidity currents are inevitably limited by scale. Since, for practical reasons, experiments at any but the smallest scales involve the use of common fluids, it is generally not possible to maintain all the dimen-

sionless parameters within ranges appropriate to modeling large-scale flows in the environment. Typically one is restricted to considering limited aspects of whole flow behavior, where the relevant parameters can be maintained within a critical range (for example, above the threshold values of the Reynolds number where similarity applies; Parsons & Garcia (1998)) and others are relaxed. Nonetheless, the use of large facilities offers scope to better define the limits to similarity. Comparable issues arise with scaling of particles and their settling velocity; the use of smaller grains may produce non-scaled surface and electrostatic effects, while the use of larger low-density grains requires higher fractional concentrations and distorts the scaling relations between particles and turbulent length scales. Problems similarly arise with non-scalable bed-forms such as ripples that are commonly generated in the laboratory. Experiments do, nonetheless, offer considerable scope for verification of numerical simulations, especially in areas such as sediment erosion mechanisms.

On the modeling side, there are substantial challenges waiting to be addressed as well. Deeper insight into the initiation process by which a slope failure evolves into a turbidity current is required to formulate suitable initial and boundary conditions for the early stages of the flow. Here the main difficulties lie in understanding the mechanisms that govern the initial fluidization of the sediment bed, a process that involves the interaction of densely packed particles that may or may not be cohesive with the interstitial fluid. Towards this end, it may be helpful to incorporate recent advances from the field of granular flows (Forterre & Pouliquen (2008), Huppert (2006), Lajeunesse et al. (2004) and references therein). Even during the later stages of the flow, the boundary layer of the turbidity current right above the bed can involve dense particle concentrations,

so that particle/particle interactions cannot be neglected. To a first order, the effects may be captured by allowing both the effective viscosity of the suspension and the particle settling velocity to depend on the local volume fraction of the particles. However, the true dynamics frequently will be substantially more complex, involving the interaction of suspended load and bedload, and the exchange of particles between the current and the bed, and possibly non-Boussinesq flow effects. Specifically, the development of advanced erosion models will be highly beneficial for improving the fidelity of numerical simulations. Once the particles are in suspension, their interaction with the fluid turbulence still involves open questions. While both experimental (Aliseda et al. (2002), and references therein) and computational (Bosse et al. (2006), and references therein) investigations of particles in homogeneous turbulence suggest that particle settling should be enhanced by two-way coupling effects, turbidity current experiments and field observations generally indicate that particles are kept in suspension by the turbulence for long times, which allows turbidity currents to travel over very long distances.

An understanding of the interaction of gravity and turbidity currents with the background stratification and the related internal wave fields is just beginning to emerge (Maxworthy et al. 2002). Similarly, the ability of turbidity currents to form topographical features on the seafloor, and their subsequent interaction with these features, should motivate further linear stability investigations and nonlinear numerical simulations. Investigations along thse lines should shed light on such issues as the meandering of channels, or the dynamics of turbidity currents propagating through sea-floor topography, where substantial reflection and wave generation may occur. Similarly, the interaction of turbidity currents with

a free surface represents a relevant research direction, due to the documented ability of near-shore slope failures and the ensuing turbidity currents to generate tsunamis (Dan et al. 2007).

Given that many hydrocarbon reservoirs consist of turbidity current deposits, it will be attractive to couple the flow simulation to a realistic substrate model for the sediment bed that accounts for spatially varying distributions of particle sizes, porosity and permeability. These properties could then feed into a reservoir model that, in turn, would form the basis of subsequent porous media flow simulations. Addressing the above goals will require the integration of complimentary research approaches from the fields of geology and fluid mechanics, involving field observations and measurements, laboratory experiments, development of fundamental models, high-resolution simulations, and linear stability analysis.

9 Future Directions

1. Improved erosion models need to be developed that can be employed in numerical simulations.
2. Researchers will have to undertake high-resolution numerical simulations that track large numbers of individual particles, in order to gain insight into the influence of particle-particle interactions.
3. The coupling between the evolution of the turbidity current and that of the underlying substrate will have to be explored.

10 Acknowledgements

EM thanks Prof. Tony Maxworthy for introducing him to the field of gravity and turbidity currents, and his Ph.D. students, postdocs and collaborators for their

contributions, especially Vineet Birman, Francois Blanchette, Peter Burns, Mike Glinsky, Esteban Gonzalez-Juez, Brendon Hall, Carlos Härtel, Leonhard Kleiser, Chris Lerch, Lutz Lesshafft, Paul Linden, James Martin, Mohamad Nasr, Frieder Necker and Moshe Strauss. Funding for this work has been provided by NASA, the National Science Foundation, BHP Billiton Petroleum and BG Group. EM furthermore gratefully acknowledges the hospitality of Prof. Greg Ivey and the Geophysical Fluid Dynamics group at the University of Western Australia during an extended visit that allowed him to focus on the writing of this article. BK acknlowledges the generous support of BG Group, and interactions with many Ph.D. students, collaborators and colleagues, notably Clare Buckee, Bill McCaffrey, Jeff Peakall, Maarten Felix, Henry Pantin and Mike Leeder. Inevitably in a paper of this type there are omissions. Some are a result of invidious choices forced by space limitations; others are mere oversights. To those whose work is not adequately acknowledged we offer our apologies.

References

1. Al-Musallami ZN, Al-Ja'aidi OS. 2008. Flow dynamics and internal velocities of experimental two-dimensional lofting density currents. *N. Jb Geol Paläont* 250:79–102

2. Aliseda A, Cartellier A, Hainaux F, Lasheras JC. 2002. Effect of preferential concentration on the settling velocity of heavy particles in homogenous isotropic turbulence. *J. Fluid Mech.* 468:77–105

3. Baas JH, McCaffrey WD, Haughton PDW, Choux C. 2005. Coupling between suspended sediment distribution and turbulence structure in a laboratory turbidity current. *J Geophys Res* 110:C11015, doi:10.1029/2004JC002668

4. Bagnold RA. 1954. Experiments on gravity free dispersion of large solid spheres in a Newtonian fluid under stress. In *Proceedings of Royal Society of London, Sem A: Math and Phys*, vol. 225

5. Bagnold RA. 1962. Auto-suspension of transported sediment: Turbidity currents. In *Proceedings of Royal Society of London, A*, vol. 265

6. Baines PG. 1995. *Topographic Effects in Stratified Flows.* Cambridge University Press

7. Benjamin TB. 1968. Gravity currents and related phenomena. *J. Fluid Mech* 31:209–48

8. Best JL, Kostaschuk RA, Peakall J, Villard PV, Franklin M. 2005. Whole flow field dynamics and velocity pulsing within natural sediment-laden underflows. *Geology* 33:765–68

9. Birman VK, Meiburg E, Kneller B. 2009. The shape of submarine levees: Exponential or power law? *J. Fluid Mech* 619:367–76

10. Blanchette F, Piche V, Meiburg E, Strauss M. 2006. Evaluation of a simplified approach for simulating gravity currents over slopes of varying angles. *Computers and Fluids* 35:492–500

11. Blanchette F, Strauss M, Meiburg E, Kneller B, Glinsky M. 2005. High-resolution numerical simulations of resuspending gravity currents: Conditions for self-sustainment. *J Geophys Res, C: Oceans* 110:C12022

12. Blum MD, Hattier-Womack J. 2009. Climate change, sea-level change and fluvial sediment supply to deepwater depositional system: A review. In *External Controls on Deepwater Depositional System*, eds. B Kneller, WD McCaffrey, OJ Martinsen. SEPM Special Publication

13. Boegman L, Ivey GN. 2009. Flow separation and resuspension beneath shoaling nonlinear waves. To appear in J Geophys Res

14. Bonnecaze RT, Huppert HE, Lister JR. 1993. Particle-driven gravity currents. *J. Fluid Mech* 250:339–69

15. Bosse T, Kleiser L, Meiburg E. 2006. Small particles in homogenous turbulence: Settling velocity enhancement by two-way coupling. *Phys Fluids* 18:027102

16. Brunner CA, Normark WR, Zuffa GG, Serra F. 1999. Deep-sea sedimentary record of the late Wisconsin cataclysmic floods from the Columbia River. *Geology* 27:463–66

17. Brunt RL, McCaffrey WD, Kneller B. 2004. Experimental modeling of the spatial distribution of grain size developed in a fill-and-spill mini-basin setting. *J Sedim Res* 74:438–46

18. Canals M, Puig P, Durrieu de Madron X, Heussner S, Palanques A, Fabres J. 2006. Flushing submarine canyons. *Nature* 444:354–57

19. Cantero MI, Balachandar S, Garcia MH. 2007. High resolution simulations of cylindrical gravity currents. *J. Fluid Mech* 590:437–69

20. Cantero MI, Garcia MH, Balachandar S. 2008. Effect of particle inertia on th dynamics of depositional particulate density currents. *Computers and Geosciences* 34:1307–18

21. Chikita K. 1989. A field study on turbidity currents initiated from spring runoffs. *Water Resources Research* 25:257–71

22. Colombini M, Parker G. 1995. Longitudinal streaks. *J. Fluid Mech* 304:161–183

23. Curray JR, Emmel FJ, Moore DG. 2003. The Bengal Fan: Morphology, geometry, stratigraphy, history and processes. *Mar and Pet Geol.* 19:1191–223

24. Dade WB, Huppert HE. 1995. A box model for non-entraining suspension-driven gravity surges on horizontal surfaces. *Sedimentology* 42:453–71

25. Dadson S, Hovius N, Pegg S, Dade WB, Horng MJ, Chen H. 2005. Hyperpycnal river flows from an active mountain belt. *J Geophys Res* 110:F04016, doi:10.1029/2004JF000244.

26. Daly RA. 1936. Origin of submarine canyons. *Am J Sci Ser* 31:401–20

27. Dan G, Sultan N, Savoye B. 2007. The 1979 Nice harbour catastrophe revisited: Trigger mechanism inferred from geotechnical measurements and numerical modeling. *Marine Geology* 245:40–64

28. De Cesare G, Schleiss A, Hermann F. 2001. Impact of turbidity currents on reservoir sedimentation. *J. Hydraul. Eng* 127:6–16

29. De Rooij F, Dalziel SB. 1998. Time- and space-resolved measurements of the deposition under turbidity currents. In *Particulate Gravity Currents*, eds. WD McCaffrey, B Kneller, J Peakall. Leeds: IAS Spec. Publ. 31

30. Dengler AT, Wilde P, Noda EK, Normark WR. 1984. Turbidity currens generated by hurricane Iwa. *Geo-Marine Letters* 4:5–11

31. Deptuck M, Piper DJW, Savoye B, Gervais A. 20008. Dimensions and architecture of the late pleistocene submarine lobes off the northern margin of east Corsica. *Sedimentology* 55:869–98

32. Eisma D, Kalf J. 1984. Dispersal of Zaire River suspended matter in the estuary and the Angola basin. *Netherlands Journal of Sea Research* 17:385–411

33. Ellison TH, Turner JS. 1959. Turbidity entrainment in stratified flows. *J Fluid Mech* 6:423–48

34. Ermanyuk EV, Gavrilov NV. 2005. Interaction of an internal gravity current with a submerged circular cylinder. *J Appl Mech Tech Phys* 46:216–23

35. Fan J. 1986. Turbid density currents in reservoirs. *Water International* 11:107–16

36. Felix M. 2002. Flow structure of turbidity currents. *Sedimentology* 49:397–419

37. Felix M, Peakall J. 2006. Transformation of debris flows into turbidity currents: Mechanisms inferred from laboratory experiments. *Sedimentology* 53:107–23

38. Ferry J, Balachandar S. 2001. A fast Eulerian method for disperse two-phase flow. *Int J Multiphase Flow* 27:1199–226

39. Flood RD. 1988. A lee wave model for deep-sea mudwave activity. *Deep Sea Res* 35:973–83

40. Forel FA. 1885. Les ravins sous-lacustres des fleuves glaciaires. *C R Acad Sci Paris* 101:725–28

41. Forterre Y, Pouliquen O. 2008. Flows of dense granular media. *Ann Rev Fluid Mech* 65:144–64

42. Garcia M, Parker G. 1993. Experiments on the entrainment of sediment into suspension by a dense bottom current. *J Geophys Res* 98:4793–807

43. Geirsdóttir A, Hardardóttir J, Sveinbjörnsdóttir AE. 2000. Glacial extent and catastrophic meltwater events during the deglaciation of southern Iceland. *Quat Sci Rev* 19:1749–61

44. Gervais A, Savoye B, Mulder T, Gonthier E. 2006. Sandy modern lobes: A new insight from high resolution seismic data. *Mar and Pet Geol.* 23:485–502

45. Girardclos S, Schmidt OT, Sturm M, Ariztegui D, Pugin A, Anselmetti FS. 2007. The 1996AD delta collapse and large turbidite in lake Brienz. *Marine Geology* 241:137–54

46. Gladstone C, Woods AW. 2000. On the application of box models to particle-laden gravity currents. *J Fluid Mech* 416:187–95

47. Gonzalez-Juez E, Meiburg E. 2009. Shallow water analysis of gravity current flows past isolated obstacles. Submitted to J Fluid Mech

48. Gonzalez-Juez E, Meiburg E, Constantinescu SG. 2008a. Gravity currents impinging on submerged cylinders: Flow fields and associated forces. Accepted for publication in J Fluid Mech

49. Gonzalez-Juez E, Meiburg E, Constantinescu SG. 2008b. The interaction of a gravity current with a circulat cylinder mounted above a wall: Effect of the gap size. Accepted for Publication in J Fluid Struct

50. Gorsline DS, De Diego T, Nava-Sanchez EH. 2000. Seismically triggered turbidites in small margin basin, western Gulf of California and Santa Monica basin, California borderland. *Sedim Geol* 135:21–35

51. Gould HR. 1951. Some quantitative aspects of Lake Mead turbidity currents. *Society of Economic Paleontologists and Mineralogists Special Publication* 2:34–52

52. Gray TE, Alexander J, Leeder MR. 2005. Quantifying velocity and turbulence structure in depositing sustained turbidity currents across breaks in slope. *Sedimentology* 52:467–88

53. Gutierrez-Pastor J, Nelson CH, Goldfinger C, Johnson JE, Escuti C, et al. 2009. Earthquake control of holocene turbidite frequency confirmed by hemipelagic sedimentation chronology on the cascadia and northen california active continental margins. In *External Controls on Deepwater Depositional System*, eds. B Kneller, WD McCaffrey, OJ Martinsen. SEPM Special Publication

54. Hacker J, Linden PF, Dalziel SB. 1996. Mixing in lock-release gravity currents. *Dyn. Atmos. Oceans* 24:183–95

55. Hall B, Meiburg E, Kneller B. 2008. Channel formation by turbidity currents: Navier-Stokes based linear stability analysis. *J Fluid Mech* 615:185–210

56. Hampton MA. 1972. The role of subaqueous debris flow in generating turbidity currents. *J Sedim Petrol* 42:775–93

57. Härtel C, Meiburg E, Necker F. 2000. Analysis and direct numerical simulation of the flow at a gravity current head. part i: Flow topology and front speed for slip and no-slip boundaries. *J Fluid Mech* 418:189

58. Heezen BC, Ewing WM. 1952. Turbidity currents and submarine slumps and the 1929 Grand Banks (Newfoundland) earthquake. *Am J Sci Ser* 250:849–73

59. Huang H, Imran J, Pirmez C. 2005. Numerical model of turbidity currents with a deforming bottom boundary. *J Hydraul Eng* 131:283–93

60. Huppert HE. 1982. The propagation of two-dimensional and axisymmetric viscous gravity currents over a rigid horizontal surface. *J Fluid Mech* 121:43–58

61. Huppert HE. 1998. Quantitative modeling of granular suspension flows. In *Trans of Royal Society of London*, vol. 356

62. Huppert HE. 2000. Geological fluid mechanics. In *Perspectices in Fluid Dynamics: A Collective Introduction to Current Research*, eds. GK Batchelor, HK Moffatt, MG Worster. Cambridge University Press

63. Huppert HE. 2006. Gravity currents: A personal perspective. *J Fluid Mech* 554:299–322

64. Huppert HE, Simpson JE. 1980. The slumping of gravity currents. *J Fluid Mech* 99:785

65. Imran J, Parker G, Pirmez C. 1999. A nonlinear model of flow in meandering submarine and subaerial channels. *J Fluid Mech* 400:295–331

66. Inman DL, Nordstrom CE, Flick RE. 1976. Currents in submarine canyons: An air-sea-land interaction. *Ann Rev Fluid Mech* 8:275–310

67. Kassem A, Imran J. 2004. Three-dimensional modeling of density current. ii flow in sinuous confined and unconfined channels. *J Hydraul Eng* 42:591–602

68. Keppie SJD, Boyle RW, Haynes SJ. 1987. Turbidite-hosted gold deposits. *Geological Assoc of Canada Special Paper* 32:186

69. Khripounoff A, Vangriesheim A, Babonneau N, Crassous P, Dennielou B, et al. 2003. Direct observation of intense turbidity current activity in the zair submarine valley at 4000 m water depth. *Marine Geology* 194

70. Kineke GC, Sternberg RW. 1995. Distribution of fluid muds on the Amazon continental shelf. *Marine Geology* 125:193–233

71. Klaucke I, Hesse R, Ryan BF. 1998. Seismic stratigraphy of the northwest Atlantic mid-ocean channel: Growth pattern of a mid-ocean channel-levee complex. *Mar and Pet Geol.* 15:575–85

72. Kneller B, Bennett SJ, McCaffrey WD. 1999. Velocity structure, turbulence and fluid stresses in experimental gravity currents. *J Geophys Res. Oceans* 104:5281–91

73. Kneller B, Buckee C. 2000. The structure and fluid mechanics of turbidity currents: A review of some recent studies and their geological implications. *Sedimentology* 47:62–94

74. Kostic S, Parker G. 2006. The response of turbidity currents to a canyon-fan

transition: Internal hydraulic jumps and depositional signatures. *J Hydraul Eng* 44:631–53

75. Kuehl SA, Brunskill GJ, Burns K, Fugate D, Kniskern T, Meneghini L. 2004. Nature of sediment dispersal off the Sepik River, Papua New Guinea: Preliminary sediment budget and implictions for margin processes. *Cont Shelf Res* 2

76. Kuenen PH. 1938. Density currents in connection with the problem of submarine canyons. *Geol Mag* 75:241–49

77. Kuenen PH. 1951. Properties of turbidity currents of high density. *Society of Economic Paleontologists and Mineralogists Special Publication* 2:14–33

78. Kuenen PH, Migliorini CI. 1950. Turbidity currents as a cause of graded bedding. *J Geol* 58:91–127

79. Lajeunesse E, Mangeney-Castelnau A, Vilotte JP. 2004. Spreading of a granular mass on a horizontal plane. *Phys Fluids* 16:2371–81

80. Lamb MP, Hickson T, Marr JG, Sheets B, Paulo C, et al. 2004. Surging versus continuous turbidity currents: Flow dynamics and deposits in an experimental intraslope minibasin. *J Sedim Res* 74:148–55

81. Lambert A, Giovanoli F. 1988. Records of riverborne turbidity currents and indications of slope failures in the Rhone delta of Lake Geneva. *Limnol. Oceanog.* 33:458–68

82. Lane-Serff GF, Beal LM, Hadfield TD. 1995. Gravity current flow over obstacles. *J Fluid Mech* 292:39–53

83. Lascelles DF. 2007. Black smokers and density currents: A uniformitarian model for the genesis of banded iron-formations. *Ore Geol Revs* 32:381–411

84. Launder BE, Rodi W. 1983. The turbulent wall jet - measurements and modeling. *Ann Rev Fluid Mech* 15:429–59

85. Lee SE, Talling PJ, Ernst GCJ, Hogg AJ. 2002. Occurence and origin of submarine plunge pools at the base of the US continental slope. *Marine Geology* 185:363–77

86. Leeder MR, Gray TE, Alexander J. 2005. Sediment suspension dynamics and a new criterion for the maintainance of turbulent suspensions. *Sedimentology* 52:683–91

87. Marcu B, Meiburg E. 1996. Three-dimensional features of particle dispersion in a nominally plane mixing layer. *Phys Fluids* 8:2266–68

88. Marcu B, Meiburg E, Newton PK. 1995. Dynamics of heavy particles in a Burgers vortex. *Phys Fluids* 7:400–10

89. Marr JG, Harff PA, Shanmugam G, Parker G. 2001. Experiments on sandy subaqueous gravity flows: The role of clay and water content in flow dynamics and depositional structures. *Geol Soc Am Bull* 113:1377–86

90. Martin JE, Meiburg E. 1994. The accumulation and dispersion of heavy particles in forced two-dimensional mixing layers. I The fundamental and subharmonic cases. *Phys Fluids* 6:1116–32

91. Mastbergen DR, Van Der Berg JH. 2003. Breaching in fine sands and the generation of sustained turbidity currents in submarine canyons. *Sedimentology* 50:625–37

92. Maxey MR, Riley JJ. 1983. Equations of motion for a small rigid sphere in a non-uniform flow. *J Fluid Mech* 28:883–89

93. Maxworthy T. 1999. The dynamics of sedimenting surface gravity currents. *J Fluid Mech* 392:27–44

94. Maxworthy T, Leilich J, Simpson JE, Meiburg E. 2002. The propagation of a gravity current into a linearly stratified fluid. *J Fluid Mech* 453:371–94

95. McCool WW, Parsons JD. 2001. Sedimentation from buoyant fine-grained suspensions. *Cont Shelf Res* 24:1129–42

96. Middleton GV. 1993. Sediment deposition from turbidity currents. *Ann Rev Earth Planet Sci* 21:89–114

97. Milliman JD, Kao SJ. 2005. Hyperpycnal discharge of fluvial sediment to the ocean: Impact of super-typhoon Herb (1996) on Taiwanese rivers. *J Geol* 113:503–06

98. Mittal R, Iaccarino G. 2005. Immersed boundary methods. *Ann Rev Fluid Mech* 37:239–61

99. Mohrig D, Marr JG. 2003. Constraining the efficiency of turbidity current generation from submarine debris flows and slides using laboratory experiments. *Mar and Pet Geol.* 20:883–99

100. Mulder T, Alexander J. 2001. The physical character of subaqueous sedimentary density flows and their deposits. *Sedimentology* 48:269–99

101. Mulder T, Syvitski J. 1995. Turbidity currents generated at river mouths during exceptional discharges to the world oceans. *J Geol* 103:285–99

102. Mulder T, Syvitski J, Migeon S, Faugeres JC, Savoye B. 2003. Marine hyperpycnal flows: Initiation, behavior and related deposits. A review. *Mar and Pet Geol.* 20:861–82

103. Nash DB. 1994. Effective sediment-transporting discharge from magnitude-frequency analysis. *J Geol* 102:79–95

104. Necker F, Härtel C, Kleiser L, Meiburg E. 2002. High-resolution simulations of particle-driven gravity currents. *Int J Multiphase Flow* 28:279–300

105. Necker F, Härtel C, Kleiser L, Meiburg E. 2005. Mixing and dissipation in particle-laden gravity currents. *J Fluid Mech* 545:339–72

106. Nelson CH, Carlson PR, Bacon CR. 1988. The Mt Mazama climactic eruption (7626 bp) and resulting convulsive sedimentation on the continent, ocean basin and Crater Lake caldera floor in Clifton. In *Sedimentologic Consequences of Convulsive Geologic Events: Geological Society of America Special Paper*, ed. HE Clifton, vol. 229

107. Nelson CH, Karabanov EB, Coleman SM. 1995. *Atls of Deep Water Environments; Architectural Style in Turbidite Systems*, chap. Late Quaternary Turbidite Systems in Lake Baikal, Russia. Smith, Chapman and Hall, 29–33

108. Nielsen P, Teakle AL. 2004. Turbulent diffusion of momentum and suspended particles: A finite-mixing-lengh theory. *Phys Fluids* 16:2342–48

109. Normark WR. 1989. Observed parameters for turbidity-current flow in channels, reserve fan, lake superior. *J Sedim Petrol* 59:423–431

110. Normark WR, Damuth DE, Wickens HDV. 1997. Sedimentary facies and associated depositional elements of the Amazon fan. In *Proceedings of the Ocean Drilling Program, Scientific Results, Leg 155*, ed. RD Flood

111. Normark WR, Piper DJW. 1991. Initiation processes and flow evolution of turbidity currents; implications for the depositional record. In *From Shoreline to*

Abyss; Contributions in Marine Geology in Honor of Francis Parker Shepard, ed. RH Osborne, vol. 46. SEPM Special Publication

112. Ogston AS, Sternberg RW, Nittrouer CA, Martin DP, Goñi MA, Crockett JS. 2008. Sediment delivery from the Fly River tidally dominated delta to the nearshore marine environment and the impact of El Niño. *J Geophys Res* 113:F01S11

113. Ooi SK, Constantinescu SG, Weber L. 2007. 2D large-eddy simultion of lock-exchange gravity current flows at high Grashof numbers. *J Hydraul Eng* 133:1037–47

114. Palanques A, Durrieu de Madron X, Puig P, Fabres J, Guillén J, et al. 2006a. Suspended sediment fluxes and transport processes in the Gulf of Lions submarine canyons. The role of storms and dense water cascading. *Marine Geology* 234:43–61

115. Palanques A, Martin J, Puig P, Guillén J, Company JB, et al. 2006b. Evidence of sediment gravity flows induced by trawling in the Palamós (Fonera) submarine canyon (northwestern Mediterranean). *Deep Sea Res* 53:201–214

116. Pan TW, Joseph DD, Bai R, Glowinski R, Sarin V. 2002. Fluidization of 1204 spheres: Simulation and experiment. *J Fluid Mech* 451:169–191

117. Pantin HM. 1979. Interaction between velocity and effective density in turbidity flow; phase-plane analysis, with criteria for autosuspension. *Marine Geology* 31:59–99

118. Pantin HM. 2001. Experimental evidence for autosuspension. In *Particulate Gravity Currents*, eds. WD McCaffrey, B Kneller, J Peakall, vol. 31. Int. Assoc. Sedim.

119. Parker G. 1982. Conditions for the ignition of catastrophically erosive turbidity currents. *Marine Geology* 46:307–27

120. Parker G, Fukushima Y, Pantin HM. 1986. Self-accelerating turbidity currents. *J Fluid Mech* 171:145–81

121. Parker G, Garcia M, Fukushima Y, Yu W. 1987. Experiments on turbidity currents over an erodible bed. *J Hydraul Eng* 52:123–47

122. Parker G, Izumi N. 2000. Purely erosional cyclic and solitary steps created by flow over a cohesive bed. *J Fluid Mech* 419:203–38

123. Parsons JD, Bush JWM, Syvitski J. 2001. Hyperpycnal plume formation from riverine outflows with small sediment concentrations. *Sedimentology* 48:465–78

124. Parsons JD, Friedrichs CT, Traykovski PA, Mohrig D, Imran J, et al. 2007. The mechanics of marine sediment gravity flows. In *Continental Margin Sedimentation: From Sediment Transport to Sequence Stratigraphy*, eds. CA Nittrouer, JA Austin, ME Field, J Syvitski, PL Wiberg

125. Parsons JD, Garcia M. 1998. Similarity of gravity current fronts. *Phys Fluids* 10:3209–13

126. Piper DJW, Cochonat P, Morrison ML. 1999. The sequence of events arounf the epicentre of the 11929 grand banks earthquake: Initiation of debris flows and turbidity currents inferred from sidescan sonar. *Sedimentology* 46:79–97

127. Piper DJW, Savoye B. 1993. Processes of late quaternary turbidity current flow and deposition on the Var deep-sea fan, northwest Mediterranean Sea. *Sedimentology* 40:3528–42

128. Prior DB, Bornhold BD, Wiseman WJ, Lowe DR. 1987. Turbidity current activity in a British Columbia fjord. *Science* 237:1330–33

129. Queney P. 1948. The problem of air flow over mountains: A summary of theoretical studies. *Bull Am Meteor Soc* 29:16–26

130. Raju N, Meiburg E. 1995. The accumulation and dispersion of heavy particles in forced two-dimensional mixing layers. II. The effect of gravity. *Phys Fluids* 7:1241–64

131. Rockwell Geyer W, Kineke GC. 1995. Observations of currents and water properties in the Amazon frontal zone. *J Geophys Res* 100:2321–39

132. Rottman JW, Linden PF. 2001. Gravity currents. In *Environmental Stratified Flows*, ed. R Grimshaw. Kluwer Academic Publishers

133. Rottman JW, Simpson JE. 1983. Gravity currents produced by instantaneous releases of heavy fluids in a rectangular channel. *J Fluid Mech* 135:95–110

134. Schmeeckle MW, Nelson JM. 2003. Direct numerical simulation of bedload transport using a local, dynamic boundary condition. *Sedimentology* 50:279–301

135. Simpson JE. 1997. *Gravity Currents: In the Environment and the Laboratory.* Cambridge University Press

136. Smith TR, Bretherton FP. 1972. Stability and the conservation of mass in drainage basin evolution. *Water Resources Research* 8:1506–29

137. Srivatsan L, Lake LW, Bonnecaze RT. 2004. Scaling analysis of deposition from turbidity currents. *Geo-Marine Letters* 24:63–74

138. Stacey MW, Brown AJ. 1988. Vertical structure of density and turbidity currents: Theory and observations. *J Geophys Res* 93:3528–42

139. Sun T, Parker G. 2005. Transportational cyclic steps created by flow over an erodible bed. Part 2. Theory and numerical simulations. *J Hydraul Eng* 43:502–14

140. Taki K, Parker G. 2005. Transportational cyclic steps created by flow over an erodible bed. Part 1. Experiments. *J Hydraul Eng* 43:488–501

141. Traykovski P, Geyer WR, Irish JD, Lynch JF. 2000. The role of wave-induced density-driven fluid mud flows for cross-shelf transport of the Eel River continental shelf. *Cont Shelf Res* 20:2113–40

142. Trofimovs J, Sparks RSJ, Talling PJ. 2008. Anatomy of a submarine pyroclastic flow and associated turbidity current: July 2003 dome collapse, Soufrière Hills volcano, Montserrat, West Indies. *Sedimentology* 55:617–34

143. Twichell DC, Schwab WC, Kenyon NH. 1995. Geometry of sandy deposits at the distal edge of the mississippi fan, gulf of mexico. In *Atls of Deep Water Environments; Architectural Style in Turbidite Systems*, eds. KT Pickering, RN Hiscott, NH Kenyon, F Ricci Lucchi, RDA Smith. London, UK: Chapman and Hall

144. Wang Z, Cheng N. 2005. Secondary flows over artificial bed strips. *Adv in Water Res* 28:441–50

145. Warrick JA, Xu J, Noble MA, Lee HJ. 2008. Rapid formation of hyperpycnal sediment gravity currents offshore of a semi-arid California river. *Cont Shelf Res* 28:991–1009

146. Weimer P, Slatt RM. 2007. Introduction to the petroleum geology of deepwater setting. In *AAPG Studies in Geology*. Tulsa, Oklahoma: American Association of Petroleum Geologists

147. Wright LD, Friedrichs CT. 2006. Gravity-driven sediment transport on continental shelves: A status report. *Cont Shelf Res* 26

148. Wright LD, Wiseman WJ, Yang ZS, Bornhold BD, Keller GH, et al. 1990. Pro-

cesses of marine dispersal and deposition of suspended silts off the modern mouth of the huanghe (yellow river). *Cont Shelf Res* 10:1–40

149. Xu JP, Noble M, Rosenfeld LK. 2004. In-situ measurements of velocity structure within turbidity currents. *Geophys Res Let* 31:L09311, doi:10.1029/2004GL019718

150. Yu B, Cantelli A, Marr J, Pirmez C, O'Byrne C, Parker G. 2006. Experiments on self-channelized subaequeous fans emplaced by turbidity currents and dilute mudflows. *J Sedim Res* 76:889–902